

# Exposing Image Resizing utilizing Welch Power Spectral Density Analysis for Double Compressed JPEG Images

Sidhant Sahu, Manish Okade

Department of Electronics and Communication Engineering,  
National Institute of Technology Rourkela  
Rourkela, India

sidhant29sahu@gmail.com, okadem@nitrkl.ac.in

## Abstract

*This paper addresses the problem of forensic analysis of recompressed images in the presence of image resizing, particularly the estimation of the resizing factor by which the image underwent resizing. The proposed method analyzes the Welch power spectral density for presence of peaks introduced by double JPEG artefacts in-order to arrive at the correct resizing factor. The correct resizing factor estimation serves as an important forensic clue since it provides vital information on the life history of the image. Experimental validation carried out utilizing several double compressed JPEG images taken from heterogeneous datasets along with comparative analysis with an existing method shows superior performance for the proposed method.*

## 1. Introduction

Authenticity of multimedia data is an important aspect in the current world since digital data is increasingly becoming a decisive element due to its admissibility in a legal framework as well as understanding the intention of the forger from a social/security point of view. This has motivated several efforts to design algorithms which check the image authenticity in a blind way. JPEG based forensics [1, 13, 10] has been attracting forensic attention since most cameras as well as image editing softwares utilize JPEG as a compression standard. Detecting multiple compressions [12, 3, 4, 2], estimating the first quantization matrix parameters [8, 5], analyzing demosaicking clues [7], analyzing resampling traces [13, 10, 11] are few research problems that have been investigated earlier with respect to JPEG based forensics. Amongst them analyzing resampling traces is an important problem since tampering often takes place by means of geometric transformations (i.e. scalings, rotations, translations) which are applied to the new content so that it could blend with the original image. This es-

sentially leaves resampling traces which could be picked up by an forensic algorithm. Resampling detection in the presence of multiple compression is the most challenging since the resampling clues tend to be destroyed by JPEG compressions thereby making detection difficult for a forensic analyst. Popesco and Farid [13] investigated a method based on detecting local spatial correlation amongst neighboring pixels which show a periodic pattern if the image has undergone resampling. However, their approach was only applicable to uncompressed TIFF images and lightly compressed JPEG images. The same limitation i.e. applicability to TIFF images was also observed in Padín et al. method [14] where subspace decomposition (SVD) along with random matrix principles were utilized to expose resampling traces. Another drawback in their method was that they were able to only analyze the upscaled scenario and downscaling was left for future work. Kirchner and Glove [10] although addressed the problem of resampling detection in presence of JPEG compression via the idea of using shifted peaks with very good detection performance yet they faced the limitation with regard to downscaling where the detection performance was observed to degrade. Bianchi and Piva [1] overcame both limitations i.e. resampling detection in presence of JPEG compression as well as better detection performance in case of downscaled images by utilizing what they referred as near lattice distribution property (NLDP) which was exploited via integer periodicity maps (IPM). Additionally, they also estimated the resizing factor as well as the quality factor of the previous JPEG compression which would provide important forensic clues. However, although NLDP gave good results yet had drawbacks like estimation of several hidden parameters, reliance on integer periodicity maps which in many cases as reported in this study gives sub-optimal results. Keeping Bianchi and Piva's [1] method as an motivation, we investigate if a better alternative to the IPM can be utilized for exposing the resampling traces in both upscaling and downscaling cases

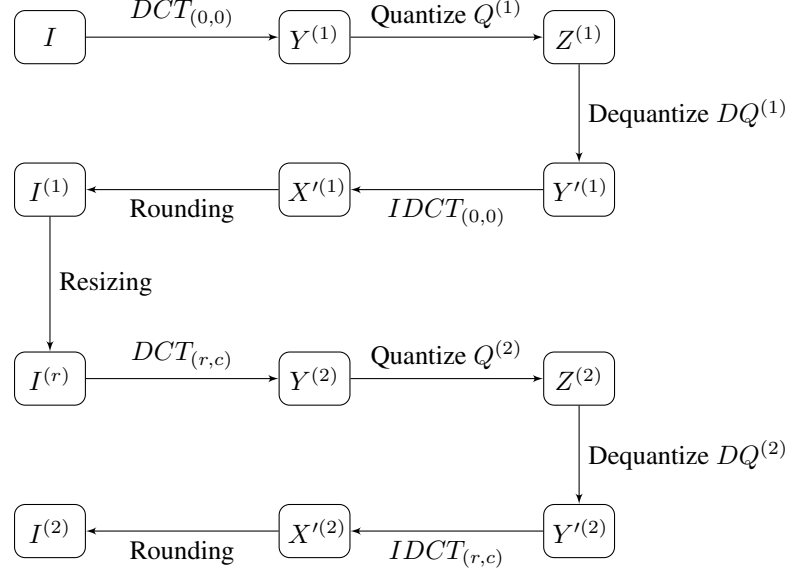


Figure 1: Double JPEG compression pipeline depicting the resizing operation between the *first*<sup>(1)</sup> JPEG and *second*<sup>(2)</sup> JPEG compression cycles.

and presence of JPEG compressions. One such analysis tool employed in this paper is the Welch Power Spectral Density (PSD) which is utilized to study the behaviour of peaks and expose resampling present in case of double JPEG scenario.

## 2. Motivation and Problem Formulation

Let  $I$  be a natural uncompressed image which we assume has not undergone any compression and resampling operation. Now let us assume that this image  $I$  is JPEG compressed with quality factor ( $QF_1$ ) followed by decompression which can be modeled as

$$I^{(1)} = IDCT_{(0,0)}(DQ(Q(DCT_{(0,0)}(I)))) = I + e_1 \quad (1)$$

In the above equation, superscript (1) denotes first compression,  $DCT_{(0,0)}$  models an  $8 \times 8$  block DCT with the grid aligned with upper left corner of the image,  $Q(\cdot)$  and  $DQ(\cdot)$  model quantization and dequantization processes, respectively and ' $e_1$ ' is the error introduced by rounding and truncating the output values to eight bit integers. Assuming that the decompressed image  $I^{(1)}$  undergoes resizing with a resizing factor denoted by ' $\xi$ ' which basically involves formation of the resampling grid with new pixel co-ordinates and estimation of the intensity values on these new pixel co-ordinates. Let us assume the resampling happens under an affine transformation of the original axes  $(n_1, n_2) \in \mathbb{Z}^2$  to  $A(n_1, n_2)^T + (\phi, \phi)^T$ , where  $A$  is the affine matrix consisting of scaling and rotation while  $(\phi, \phi)^T$  is the translation vector. In this paper only scaling is analyzed (i.e. resizing with factor of  $\xi$ ) hence we assume the rotation angle and translation parameter to be set to 0. Under this assumption

the affine matrix can be written as  $A = \xi I_2$  where  $I_2$  is  $2 \times 2$  identity matrix and  $\xi \triangleq \frac{L}{M}$  with  $(L, M) \in \mathbb{N}^+$ . If  $\xi < 1$  the resizing results in downscaling and  $\xi > 1$  results in upscaling. Mathematically, the entire process can be modeled using new resampling grid  $(m_1, m_2)$  and estimation of the intensity values on  $(m_1, m_2)$  which can be performed with a  $2 - D$  separable linear symmetric interpolation kernel denoted by  $h(n_1, n_2)$  i.e.

$$\begin{aligned} I^r(m_1, m_2) &= h(n_1, n_2) * I^{(1)}(n_1, n_2) \\ &= \sum_{\forall n_1 \in Z} \sum_{\forall n_2 \in Z} h(\xi^{-1}m_1 - n_1) h(\xi^{-1}m_2 - n_2) \\ &\quad I^{(1)}(n_1, n_2) \\ &= \sum_{\forall n_1 \in Z} \sum_{\forall n_2 \in Z} h\left(\frac{M}{L}m_1 - n_1\right) h\left(\frac{M}{L}m_2 - n_2\right) \\ &\quad I^{(1)}(n_1, n_2) \end{aligned} \quad (2)$$

Now assuming the resized image ' $I^r$ ' undergoes second JPEG compression with quality factor ( $QF_2$ ) and DCT grid aligned with upper left corner of the resized image which indicates there is no misalignment ( $r, c = 0$ ) between the two compressions i.e.

$$\begin{aligned} I^{(2)} &= IDCT_{(r,c)}(DQ(Q(DCT_{(r,c)}(I^r)))) \\ &= I^r(m_1, m_2) + e_2 \end{aligned} \quad (3)$$

In the above equation, superscript (2) denotes second compression and  $I^{(2)}$  henceforth would be referred as DCR

(double compressed and resized) image. This entire process is depicted in Figure 1. Our study shows that the error terms present in Eq. (1) and Eq. (3) due to the rounding and truncation operations manifests themselves as peaks in the power spectrum when the histogram of DC coefficients is analyzed in the block DCT domain. For the single compressed image (Eq. (1)), a prominent peak in the power spectrum is observed due to the ' $e'_1$ ' term. If resizing occurred after the first compression cycle then as modeled by Eq. (2) it would be an estimation of the intensity values on the new pixel co-ordinates via an interpolation filter (ideally sinc pulse) which filters out the error components that fall outside the frequency range  $[-\xi\pi, \xi\pi]$  thereby eliminating the peak in the power spectrum which was earlier present in the single compressed image. Post-resizing if the image undergoes second JPEG compression/decompression i.e. Eq.(3) then again there would be reappearance of peak in the power spectrum due to the error term ' $e'_2$ '. The behavior of the error terms in the form of peaks serve as a clue which is exploited in this study as follows. Since it is not known by what resizing factor the DCR image underwent resizing, the objective is to estimate the correct resizing factor amongst several possible candidate resizing factors for which the behavior of the error terms in the form of peaks is exploited. Towards this goal, the DCR image under analysis is reverse resized utilizing a set of candidate resizing factors followed by analyzing the Welch power spectral density (PSD) for traces of resizing in the form of peaks. Figure 2 shows the PSD plot for reverse resized DCR image where 5 candidate reverse resizing factors  $\xi = \{0.6, 0.8, 0.9, 1.1, 1.3\}$  are utilized. Observations from Figure 2 show reverse resizing by the inverse of true resizing factor nullifies the effect of the error term ' $e'_2$ ' in Eq. (3) due to interpolation filter and brings back the behavior of ' $e'_1$ ' term which manifests itself as a prominent peak ( $\xi = 0.8$  in this case) which is the premise of the proposed method. The motivation of utilizing Welch method is that it analyzes the PSD at different frequencies. Since Welch method applies a bandpass filter with center frequency tuned to the frequency of interest along with optimum bandwidth decided by segment length, it kind of averages and smoothes the underlying behavior of the peaks thereby revealing the diagnostic peak in the PSD again (when reverse resized by the inverse of the true resizing factor) which had got lost in the resizing attack.

### 3. Key Contributions

In this work, the Welch power spectra is utilized to study the behaviour of peaks introduced by the double JPEG artefacts in the presence of resizing (i.e. up-scaled and down-scaled). The objective is to estimate the true resizing factor by which the DCR image underwent resizing which is achieved by reversing the resizing operation utilizing a set

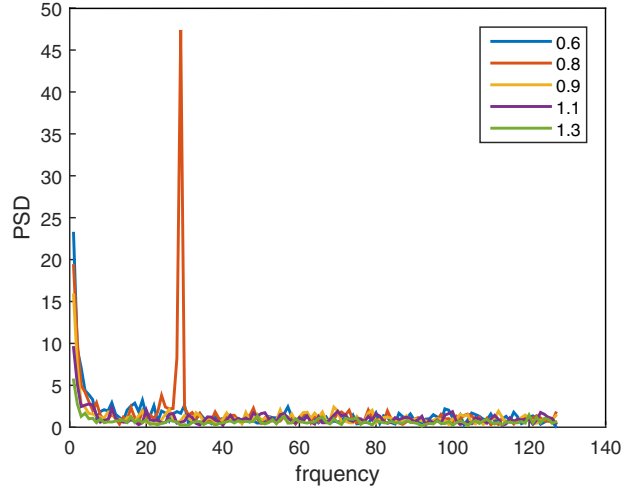


Figure 2: Power spectral density plot for reverse resized DCR image depicting 5 reverse resizing factors (image big169.tiff taken from Pivas database doubly compressed with  $QF_1 = 70$ ,  $QF_2 = 90$  and resized by  $\xi = 0.8$ )

of candidate resizing factor followed by testing whether the histogram of DC coefficient shows periodicity due to the quantization operated by the first compression in the Welch power spectra. Experimental results demonstrate that this idea of utilizing Welch periodogram is found to be superior as compared to the existing DFT based peak detector utilized by Bianchi and Piva [1].

### 4. Proposed Method

The premise of the proposed method is based on utilizing the traces of resizing present in the Welch power spectral density of the histogram of DC coefficients when  $8 \times 8$  block DCT is applied to the image under analysis. As outlined earlier a prominent peak would be present in the Welch PSD estimate for the image which would be reverse resized with the true resizing factor. The proposed method is detailed below;

1. Choose the candidate resizing factors utilizing either a fixed finite set  $\xi = \{0.6, 0.7, 0.8, 0.9, 0.95, 1.05, 1.1, 1.2, 1.3, 1.4\}$  or utilizing an estimation algorithm given in [1].
2. Utilizing each of the candidate resizing factors ( $\xi$ ), perform reverse resizing ( $\gamma = \xi^{-1}$ ) of the DCR image with interpolation set to bicubic.
3. For each reverse resized image, firstly apply  $8 \times 8$  block DCT and form the histogram of the DC coefficients. The obtained histogram sequence  $(x(l), l \in (0, L-1))$  is analyzed further as described below;

(a) Partition the histogram sequence into ' $K$ ' overlapping segments, each segment having length ' $P'$ . Let ' $Q$ ' denote the new points which appear in the subsequent segments. Therefore, the number of points common to two adjacent segments is denoted by  $(P - Q)$  and the % overlap is estimated using  $\left( \frac{P - Q}{P} \times 100 \right)$

(b) Compute the windowed DFT for each of the ' $K$ ' segments using the window function  $w(p)$

$$X_k(f) = \sum_p x(p)w(p)\exp(-j2\pi fp) \quad (4)$$

(c) Compute the Welch estimate of PSD utilizing

$$S_x(f) = \frac{1}{K} \sum_{k=1}^K \frac{1}{W} |X_k(f)|^2 \quad (5)$$

$$\text{where, } W = \sum_{p=1}^P w^2(p)$$

(d) Pick the prominent peak present in the Welch estimate of PSD utilizing

$$G \triangleq \max_f(S_x(f)) \quad (6)$$

4. Analyze the peaks and choose the resizing factor yielding the most prominent peak amongst all the candidate resizing factors i.e.

$$G_{(\xi=\gamma^{-1})} \triangleq \max_\gamma(G_\gamma) \quad (7)$$

## 5. Results and Discussions

MATLAB 2014b is used for experimentation. The proposed method is tested on images taken from three different datasets namely RAISE [6], DRESDEN [9] and Bianchi and Piva's dataset. 90 uncompressed images (in TIFF format) of size  $1024 \times 1024$  are picked (30 images from each dataset) from these datasets followed by compressing them with five different JPEG quality factors  $QF_1 \in (50, 60, 70, 80, 90)$  to form the singly compressed images. Now, each singly compressed image is resized (using 'imresize') by utilizing the resizing factors from the candidate set of size 10 i.e.  $\xi = \{0.6, 0.7, 0.8, 0.9, 0.95, 1.05, 1.1, 1.2, 1.3, 1.4\}$  with bi-cubic interpolation. The single compressed resized images are compressed again with six different quality factors  $QF_2 \in (50, 60, 70, 80, 90, 99)$  to form a total of 27000 ( $90 \times 5 \times 10 \times 6$ ) double compressed resized images. The experiment is carried out on luma component of the central square block of size  $512 \times 512$ . The reverse

resized images have been obtained utilizing resizing factors coming from either an estimation algorithm [1] which we henceforth refer to as '*estimated*' or from a fixed candidate set of size ten which we henceforth refer to as '*fixed*'. For both cases 'imresize' is used along with bi-cubic interpolation. For Welch analysis, the segment length ' $P$ ' is set to 256 points and 50% overlap is taken between adjacent segments. The power spectrum is analyzed for frequencies  $f = \frac{i}{p}$  with  $-(\frac{p}{2} - 1) \leq i \leq \frac{p}{2}$  and rectangular window is being used as window function. Comparative analysis is carried out with integer periodicity map (IPM) method of Bianchi and Piva [1], where integer periodicity map is utilized as a measure of the NLDP. The motivation for choosing Bianchi and Piva's method is that it also utilizes a similar property as PSD namely NLDP, which we show in this study is sub-optimal and dependent on a lot of hidden parameters. Further, this research work is carried out in a reproducible manner and the MATLAB code needed to reproduce the presented results is made available at our research group's webpage <https://sites.google.com/site/manishokade/publications> with the motivation that it will be useful to fellow researchers.

### 5.1. Quantitative analysis

The efficiency of proposed method is evaluated by measuring the percentage of correct resizing factor estimation which is defined as the number of DCR images for which the proposed algorithm gives the correct resizing factor over all DCR images. Additionally, the Mean Absolute Error (MAE) is also analyzed in order to quantify the proposed method. For the '*fixed*' case, we considered the estimated resizing factor ( $\hat{\xi}$ ) as true resizing factor ( $\xi$ ) if  $|\hat{\xi} - \xi| = 0$  while for the '*estimated*' case we used  $|\hat{\xi} - \xi| < 0.05$ . Figure 3(a)(b) shows the plot for percentage of correct resizing factor estimates obtained for the proposed method (utilizing estimated as well as fixed resizing factors) along with its comparative analysis with IPM method [1]. Figure 3(a) depicts the analysis carried out for different resizing factors considering second JPEG quality factor ( $QF_2$ ) fixed at 90 and averaged over the first JPEG quality factor  $QF_1$  range. As observed from Figure 3(a) the performance of the proposed method is superior to the IPM method specifically in the downscaling scenario signifying that analyzing the subtle traces of resizing via the Welch PSD is better able to arrive at the correct resizing factor. Figure 3(b) shows the performance analysis for different second JPEG quality factor ( $QF_2$ ), averaged over the ( $QF_1$ ) range as well as averaged over all resizing factors. As observed from Figure 3(b) as  $QF_2$  increases, the performance increases indicating that at lower quality factors of the second compression the clues left behind are erased due to the effects of the quantization (division by large values).

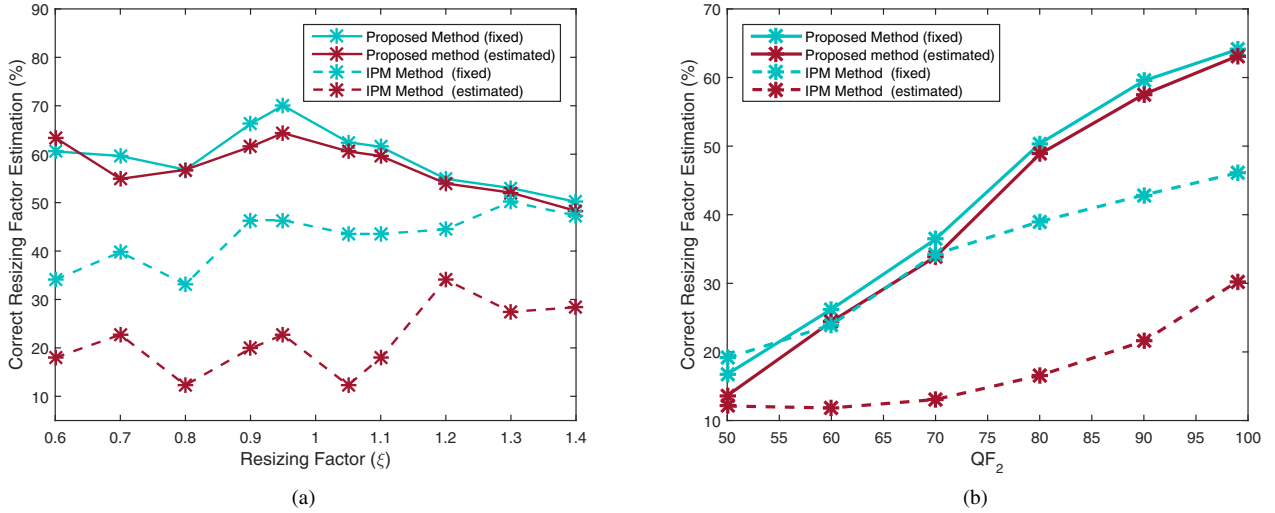


Figure 3: Correct resizing factor estimation (%) for (a) different resizing factors  $\xi$ , considering  $QF_2 = 90$  and  $QF_1 \in (50, \dots, 90)$  (b) different quality factors  $QF_2$ , averaged over all resizing factors ( $\xi$ ) and  $QF_1 \in (50, \dots, 90)$ . Solid lines denote proposed method while dashed lines denote IPM method. Green color is used to depict the 'fixed' case while maroon color is used to depict the 'estimated' case.

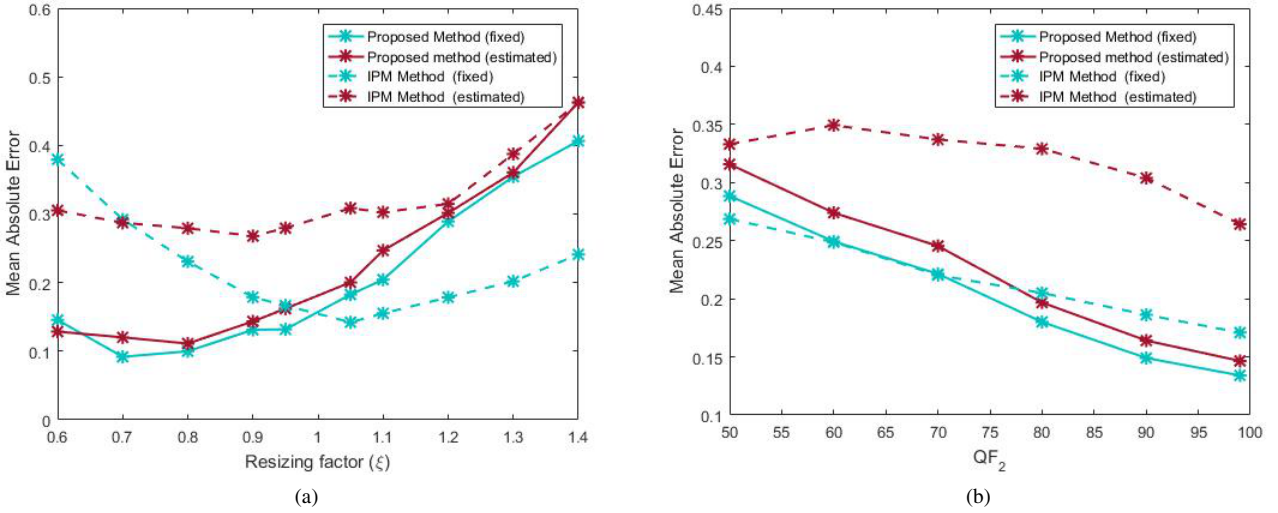


Figure 4: Mean Absolute Error (MAE) performance for (a) different resizing factors ( $\xi$ ), averaged over all  $QF_2$  and  $QF_1 \in (50, \dots, 90)$  (b) different  $QF_2$ , averaged over all resizing factors ( $\xi$ ) and  $QF_1 \in (50, \dots, 90)$ . Solid lines denote proposed method while dashed lines denote IPM method. Green color is used to depict the 'fixed' case while maroon color is used to depict the 'estimated' case.

Figure 4(a)(b) shows the Mean Absolute Error obtained for the proposed method along with its comparative analysis with IPM method [1]. Figure 4(a) analyzes its variation with respect to different resizing factors averaged over  $QF_2$  as well as averaged over  $QF_1$  while Figure 4(b) analyzes

its variation with respect to  $QF_2$  averaged over all resizing factors as well as  $QF_1$  ranges. As observed, the proposed method achieves lower error rate especially in the downscaling cases due to absence of aliasing since reverse resizing by the inverse of the correct resizing factor negates

Table 1: Correct resizing factor estimation (%) achieved by the proposed algorithm for  $\xi = 0.6$  averaged over all  $QF_2$  and  $QF_1$ . (*fixed case*)

|        |    | $QF_2$ |       |       |       |       |       |
|--------|----|--------|-------|-------|-------|-------|-------|
|        |    | 50     | 60    | 70    | 80    | 90    | 99    |
| $QF_1$ | 50 | 48.61  | 48.61 | 50    | 84.72 | 91.66 | 97.22 |
|        | 60 | 47.22  | 48.61 | 50    | 68.05 | 91.66 | 95.83 |
|        | 70 | 47.22  | 50    | 47.22 | 47.22 | 66.67 | 77.78 |
|        | 80 | 50     | 47.22 | 48.61 | 45.83 | 48.61 | 48.61 |
|        | 90 | 48.61  | 50    | 47.22 | 45.83 | 48.61 | 48.61 |

Table 2: Correct resizing factor estimation (%) achieved by IPM Method for  $\xi = 0.6$  averaged over all  $QF_2$  and  $QF_1$ . (*fixed case*)

|        |    | $QF_2$ |       |       |       |       |       |
|--------|----|--------|-------|-------|-------|-------|-------|
|        |    | 50     | 60    | 70    | 80    | 90    | 99    |
| $QF_1$ | 50 | 2.77   | 11.11 | 38.89 | 63.89 | 79.17 | 75    |
|        | 60 | 2.77   | 1.38  | 5.56  | 52.78 | 77.78 | 80.56 |
|        | 70 | 5.56   | 4.17  | 5.56  | 6.95  | 13.89 | 22.23 |
|        | 80 | 8.33   | 13.89 | 4.17  | 9.72  | 8.33  | 13.89 |
|        | 90 | 8.33   | 4.17  | 9.72  | 8.33  | 6.94  | 11.11 |

the noise components. A common observation from Figure 3 and Figure 4 for both methods is that the 'fixed candidate case' is easy to estimate in comparison to the 'estimated case' due to the errors present in the estimation algorithm utilized to arrive at the candidate resizing factors. Finally, Table 1 and Table 2 shows the performance achieved by the proposed as well as the IPM method at a particular resizing factor ( $\xi = 0.6$ ), averaged over all  $QF_2$  and  $QF_1$ . Observations from both tables reveal significant outperformance by the proposed method in comparison to IPM method indicating that PSD serves as vital tool to analyze the forensic clues left over by the resizing operation.

## 6. Conclusions

This paper investigated the forensic analysis of double compressed JPEG images with respect to the image resizing problem. Of particular interest in this study was the estimation of the correct resizing factor which had been applied between two successive JPEG compression cycles. This was carried out utilizing the Welch power spectral density by analyzing the peaks and choosing the resizing factor which gave the most prominent peak amongst the candidate resizing factors. Comparative analysis carried out with an existing state-of-the-art method show superior performance for the proposed method.

## References

- [1] T. Bianchi and A. Piva. Reverse engineering of double jpeg compression in the presence of image resizing. In *IEEE International Workshop on Information Forensics and Security (WIFS)*, pages 127–132, Dec 2012. 1, 3, 4, 5
- [2] C. Chen, J. Ni, Z. Shen, and Y. Q. Shi. Blind forensics of successive geometric transformations in digital images using spectral method: Theory and applications. *Trans. Img. Proc.*, 26(6):2811–2824, June 2017. 1
- [3] X. Chu, Y. Chen, M. C. Stamm, and K. J. R. Liu. Information theoretical limit of compression forensics. In *IEEE International Conference on Acoustics, Speech and Signal Processing (ICASSP)*, pages 2689–2693, May 2014. 1
- [4] V. Conotter, P. Comesaa, and F. Prez-Gonzlez. Forensic detection of processing operator chains: Recovering the history of filtered jpeg images. *IEEE Transactions on Information Forensics and Security*, 10(11):2257–2269, Nov 2015. 1
- [5] N. Dalmia and M. Okade. Robust first quantization matrix estimation based on filtering of recompression artifacts for non-aligned double compressed JPEG images. *Sig. Proc.: Image Comm.*, 61:9–20, 2018. 1
- [6] D.-T. Dang-Nguyen, C. Pasquini, V. Conotter, and G. Boato. Raise: A raw images dataset for digital image forensics. In *Proceedings of the 6th ACM Multimedia Systems Conference, MMSys ’15*, pages 219–224, New York, NY, USA, 2015. ACM. 4
- [7] P. Ferrara, T. Bianchi, A. D. Rosa, and A. Piva. Image forgery localization via fine-grained analysis of cfa artifacts. *IEEE Transactions on Information Forensics and Security*, 7(5):1566–1577, Oct 2012. 1
- [8] F. Galvan, G. Puglisi, A. R. Bruna, and S. Battiatto. First quantization matrix estimation from double compressed JPEG images. *IEEE Transactions on Information Forensics and Security*, 9(8):1299–1310, Aug 2014. 1
- [9] T. Gloe and R. Bhme. The 'Dresden Image Database' for benchmarking digital image forensics. In *Proceedings of the 25th Symposium On Applied Computing (ACM SAC 2010)*, volume 2, pages 1585–1591, 2010. 4
- [10] M. Kirchner and T. Gloe. On resampling detection in recompressed images. In *First IEEE International Workshop on Information Forensics and Security (WIFS)*, pages 21–25, Dec 2009. 1
- [11] J. Kodovsky and J. Fridrich. Effect of image downsampling on steganographic security. *IEEE Transactions on Information Forensics and Security*, 9(5):752–762, May 2014. 1
- [12] T. Pevny and J. Fridrich. Detection of double-compression in jpeg images for applications in steganography. *IEEE Transactions on Information Forensics and Security*, 3(2):247–258, June 2008. 1
- [13] A. C. Popescu and H. Farid. Exposing digital forgeries by detecting traces of resampling. *IEEE Transactions on Signal Processing*, 53(2):758–767, Feb 2005. 1
- [14] D. Vzquez-Padn, F. Prez-Gonzlez, and P. Comesaa-Alfaro. A random matrix approach to the forensic analysis of upscaled images. *IEEE Transactions on Information Forensics and Security*, 12(9):2115–2130, Sept 2017. 1